

---

---

# <sup>64</sup>Cu-Intraperitoneal Radioimmunotherapy: A Novel Approach for Adjuvant Treatment in a Clinically Relevant Preclinical Model of Pancreatic Cancer

Yukie Yoshii<sup>1</sup>, Hiroki Matsumoto<sup>2</sup>, Mitsuyoshi Yoshimoto<sup>3</sup>, Yoko Oe<sup>1</sup>, Ming-Rong Zhang<sup>1</sup>, Kotaro Nagatsu<sup>1</sup>, Aya Sugyo<sup>1</sup>, Atsushi B. Tsuji<sup>1</sup>, and Tatsuya Higashi<sup>1</sup>

<sup>1</sup>National Institute of Radiological Sciences, National Institutes for Quantum and Radiological Science and Technology, Chiba, Japan; <sup>2</sup>Nihon Medi-Physics Co., Ltd., Chiba, Japan; and <sup>3</sup>Division of Functional Imaging, National Cancer Center Hospital East, Chiba, Japan

---

Pancreatic cancer (PC) has a very poor prognosis. Surgery is the primary treatment for patients with resectable PC; however, local recurrence, hepatic metastasis, and peritoneal dissemination often occur even after extensive surgery. Adjuvant chemotherapy, typically with gemcitabine, has been used clinically but with only a modest survival benefit. To achieve a better outcome, we investigated the efficacy of <sup>64</sup>Cu-intraperitoneal radioimmunotherapy (ipRIT) with <sup>64</sup>Cu-labeled antiepidermal growth factor receptor antibody cetuximab as an adjuvant treatment after PC surgery using an orthotopic xenografted mouse model. **Methods:** The efficacy of adjuvant <sup>64</sup>Cu-ipRIT was investigated in a human PC mouse model harboring orthotopic xenografts of xPA-1-DC cells. To reproduce the clinical situation, PC xenografts were surgically resected when pancreatic tumors were readily visible but not metastatic tumors. Increasing doses of <sup>64</sup>Cu-cetuximab were intraperitoneally injected, and the mice were monitored for toxicity to determine the safe therapeutic dose. For adjuvant <sup>64</sup>Cu-ipRIT, the day after tumor resection, the mice were intraperitoneally administered 22.2 MBq of <sup>64</sup>Cu-PCTA-cetuximab and the survival was compared with that in surgery-only controls. For comparison, adjuvant chemotherapy with gemcitabine was also examined using the same model. **Results:** The mouse model not only developed primary tumors in the pancreas but also subsequently reproduced local recurrence, hepatic metastasis, and peritoneal dissemination after surgery, which is similar to the manifestations that occur with human PC. Adjuvant <sup>64</sup>Cu-ipRIT with <sup>64</sup>Cu-labeled cetuximab after surgery effectively suppressed local recurrence, hepatic metastasis, and peritoneal dissemination in this model. Significant improvement of the survival with minimal toxicity was achieved by adjuvant <sup>64</sup>Cu-ipRIT compared with that in control mice that underwent surgery only. Adjuvant chemotherapy with gemcitabine nominally prolonged the survival, but the effect was not statistically significant. **Conclusion:** <sup>64</sup>Cu-ipRIT with cetuximab can be an effective adjuvant therapy after PC surgery.

**Key Words:** adjuvant therapy; <sup>64</sup>Cu-intraperitoneal radioimmunotherapy; pancreatic cancer; orthotopic model; <sup>64</sup>Cu-labeled cetuximab

**J Nucl Med 2019; 60:1437–1443**  
DOI: 10.2967/jnumed.118.225045

---

**P**atients with pancreatic cancer (PC) have a very poor prognosis, with an overall 5-y survival rate below 5% (1). Surgical resection is the primary treatment for patients with resectable PC without obvious metastasis; however, local recurrence, hepatic metastasis, and peritoneal dissemination are frequently observed even after extensive surgery (2). These recurrences are thought to stem from minimal undetectable metastases that were present at the time of surgery (2). To improve the survival of PC patients after resection, adjuvant chemotherapy, typically with gemcitabine, has been used clinically. The large phase III study CONKO-001 showed that adjuvant chemotherapy with gemcitabine significantly prolonged median overall survival (22.8 mo vs. 20.2 mo in the surgery-only group) (3); however, most patients died within 2 y after the surgery. The phase III study JSAP-02 reported that adjuvant chemotherapy with gemcitabine tended to prolong median overall survival (22.3 mo vs. 18.4 mo in the surgery-only group), but the difference was not statistically significant (4). Therefore, more effective adjuvant therapies are required to treat PC.

Toward this end, we have focused on intraperitoneal radioimmunotherapy (ipRIT) using a radiolabeled tumor-specific binding antibody. Intraperitoneal injection of radiolabeled antibodies ensured higher and more rapid accumulation in peritoneal dissemination, leading to prolonged survival in mice compared with intravenous injection (5–8). Additionally, intraperitoneal, rather than intravenous, administration of a tumor-specific binding antibody resulted in greater accumulation in pancreatic tumors in an orthotopic mouse model, in early pancreatic ductal adenocarcinoma in a spontaneous mouse model (9), and in hepatic metastases in mice (10). These pieces of evidence support the applicability of ipRIT as an adjuvant treatment for PC.

Several therapeutic radioisotopes for ipRIT have been used to date, such as the  $\beta^-$  emitters <sup>131</sup>I and <sup>177</sup>Lu or the  $\alpha$  emitter <sup>225</sup>Ac (5–7). However, the sustainable use of a nuclear reactor for the production of <sup>131</sup>I and <sup>177</sup>Lu is a key challenge for future clinical practice, and the availability of <sup>225</sup>Ac obtained by radiochemical

---

Received Dec. 25, 2018; revision accepted Feb. 20, 2019.  
For correspondence contact: Yukie Yoshii, National Institute of Radiological Sciences, National Institutes for Quantum and Radiological Science and Technology, 4-9-1 Anagawa, Inage, Chiba 263-8555, Japan.  
E-mail: yoshii.yukie@qst.go.jp.  
Published online Mar. 8, 2019.  
COPYRIGHT © 2019 by the Society of Nuclear Medicine and Molecular Imaging.

extraction from  $^{229}\text{Th}$  is still limited (11–13). As a potential alternative,  $^{64}\text{Cu}$  ( $\beta^-$  decay, 0.574 MeV, 40%; electron capture, 42.6%;  $\beta^+$  decay, 0.653 MeV, 17.4%) might be used as a radioisotope for ipRIT.  $^{64}\text{Cu}$  was shown to effectively prolong survival in mouse models with peritoneal dissemination (8) and can easily be produced on a large scale (14).  $\beta^-$  particles and high-linear-energy-transfer Auger electrons emitted from  $^{64}\text{Cu}$  can highly damage tumor cells (15). The first-in-human study of  $^{64}\text{CuCl}_2$  radionuclide therapy was recently conducted, suggesting the potential of  $^{64}\text{Cu}$  for clinical use (16).

Additionally, the effectiveness of the  $^{64}\text{Cu}$ -labeled anti-epidermal growth factor receptor (EGFR) antibody cetuximab for PET imaging and internal radiotherapy has been well established in many preclinical studies (17,18). We previously showed that ipRIT with  $^{64}\text{Cu}$ -labeled cetuximab was effective in peritoneal-dissemination mouse colorectal and gastric cancer cells (HCT116-RFP and NUGC4-RFP) and that the estimated absorbed doses to normal organs in humans were sufficiently low relative to the reported tolerance doses (8). Since cetuximab has high binding affinity for EGFR, which is overexpressed in up to 90% of PCs (19), we hypothesized that  $^{64}\text{Cu}$ -ipRIT with the  $^{64}\text{Cu}$ -labeled cetuximab would be an effective adjuvant treatment after surgery in PC. As a proof of concept, we tested the effectiveness of adjuvant  $^{64}\text{Cu}$ -ipRIT with cetuximab using a clinically relevant orthotopic PC xenograft mouse model.

## MATERIALS AND METHODS

### Preparation of $^{64}\text{Cu}$ -Labeled Cetuximab

Cetuximab was obtained from Merck Serono.  $^{64}\text{Cu}$  was produced and purified using previously published methods (14). Cetuximab was  $^{64}\text{Cu}$ -labeled with the chelator 3,6,9,15-tetraazabicyclo[9.3.1]pentadecan-1(15),11,13-triene-3,6,9-triacetic acid (PCTA), since previous studies using PCTA for  $^{64}\text{Cu}$  labeling with cetuximab showed a high radiolabeling yield and in vitro serum stability (8,18).  $^{64}\text{Cu}$ -PCTA-cetuximab was prepared according to the methods described in our previous study (8), with the specific activity ranging from 1.1 to 1.7 GBq/mg. In animal experiments, the injected protein dose of  $^{64}\text{Cu}$ -PCTA-cetuximab was adjusted to 20  $\mu\text{g}$  per mouse by adding an unlabeled antibody as reported previously (8,20).

### Cell Culture and Establishment of the Clinically Relevant Orthotopic PC Xenograft Mouse Model

Human PC xPA-1 cells expressing red fluorescent protein in the cytoplasm and green fluorescent protein in the nucleus (xPA-1-dual color, xPA-1-DC) were obtained from AntiCancer. xPA-1-DC cells were cultured in RPMI-1640 medium (Wako) supplemented with 10% fetal bovine serum in a humidified atmosphere of 95% air and 5%  $\text{CO}_2$  at 37°C.

All animal experiments were approved by the Animal Ethics Committee of our institutions and conducted in accordance with the institutional guidelines. Six-week-old female BALB/c nude mice were obtained from Japan SLC. The xPA-1-DC cells ( $5 \times 10^6$ ) in 25  $\mu\text{L}$  of RPMI-1640 medium mixed with 25  $\mu\text{L}$  of ice-cold Matrigel matrix (BD Biosciences) were injected into the pancreatic tail through the incision. For surgical resection of primary PC, partial pancreatectomy and splenectomy were performed as described previously (21) at 7 d after tumor cell inoculation, since their primary tumors were sufficiently visible in the pancreas but obvious metastases were not yet apparent at this time point. The optimal timing of the surgical resection of PC was determined by sacrificing the mice at 7 and 9 d after tumor cell inoculation, and primary tumor growth and metastases were observed in 5 animals per time point. In this study, tumor development and recurrences were observed with the aid of a stereoscopic fluorescence microscope (8). The pattern of postoperative recurrence was

examined with the model mice sacrificed at 2 wk after surgical resection ( $n = 9$ ).

### Histopathology and Immunohistochemistry

Harvested tumors and tissues were fixed in 10% buffered formalin (Sigma-Aldrich) at room temperature and processed for paraffin embedding, and sections at a 6- $\mu\text{m}$  thickness were obtained according to standard histologic procedures. Immunohistochemical staining for EGFR was performed with deparaffinized sections according to previously described methods (8). Primary antibodies against EGFR (1:50 dilution; Cell Signaling Technology) and rabbit IgG isotype for negative control were used. Immunohistochemistry sections were counterstained with hematoxylin. Images were obtained with an Olympus BX43 microscope with a DP21 camera system (Olympus).

### Toxicity Characterization

Before the treatment study, the effect of the intraperitoneally injected  $^{64}\text{Cu}$ -PCTA-cetuximab (0, 11.1, 22.2, 37, 74 MBq; 4–5/group) on body weight and on hematologic and biochemical parameters was examined to determine the therapeutic dose. Body weight was measured on day 0 (just before  $^{64}\text{Cu}$ -PCTA-cetuximab injection) and on days 3, 7, 9, 14, 17, 21, 24, 28, and 35. Hematologic parameters were measured on day 0 (just before  $^{64}\text{Cu}$ -PCTA-cetuximab injection) and on days 7, 14, 21, 28, and 35, using blood collected from the tail vein. The concentrations of white blood cells, red blood cells, and platelets were determined using a hematologic analyzer (Celltac MEK-6458; Nihon Kohden). Biochemical parameters were measured on day 35 in mouse plasma prepared from blood collected by cardiac puncture. The levels of glutamate oxaloacetate transaminase, glutamate pyruvate transaminase, and alkaline phosphatase were determined to assess liver function. Blood urea nitrogen and creatinine levels were determined to assess kidney function. Amylase and lipase levels were determined to assess pancreas function. Biochemical parameters were measured using a blood biochemistry analyzer (Dri-Chem 7000VZ; Fuji Film). Given that the hematologic and biochemical parameters of mice administered  $^{64}\text{Cu}$ -PCTA-cetuximab intraperitoneally at doses of 22.2 and 37 MBq had been examined in a similar manner in our previous study (8), those data were included for analysis in the present study.

### Tumor Uptake

To characterize uptake of  $^{64}\text{Cu}$ -PCTA-cetuximab into xPA-1-DC orthotopic xenografts, accumulation of  $^{64}\text{Cu}$ -PCTA-cetuximab at 24 h after intraperitoneal injection was evaluated and compared with the values obtained in the similar manner in the intraperitoneal HCT116-RFP colon cancer tumors and in the normal pancreas of tumor-free mice as reported by us previously (8). Mice with orthotopic xenografts of xPA-1-DC cells at 7 days after cell inoculation were injected intraperitoneally with 7.4 MBq  $^{64}\text{Cu}$ -PCTA-cetuximab ( $n = 8$ ) and killed at 24 h after injection. Tumors were isolated and weighed. Radioactivity levels were measured with a  $\gamma$ -counter (1480 Wizard 3 automatic  $\gamma$ -counter; PerkinElmer). The percentage injected dose per gram was calculated.

### Adjuvant $^{64}\text{Cu}$ -ipRIT After PC Resection

For the in vivo treatment, the mice with xPA-1-DC orthotopic xenografts were randomized into 2 groups at 7 d after cell inoculation: adjuvant  $^{64}\text{Cu}$ -ipRIT and surgery-only (control) groups (10/group). In both groups, surgical resection of primary PC was performed. One day after the surgery, the mice were injected intraperitoneally with 22.2 MBq of  $^{64}\text{Cu}$ -PCTA-cetuximab (adjuvant  $^{64}\text{Cu}$ -ipRIT group) or saline (surgery-only control group) at day 0. After the toxicity characterization, we chose to perform adjuvant  $^{64}\text{Cu}$ -ipRIT with 22.2 MBq of  $^{64}\text{Cu}$ -PCTA-cetuximab per mouse because this was the maximum

dose that did not show any significant toxicity. Mice were monitored for mortality until day 83, and the evaluation was performed as previously reported (8). Mice were sacrificed at a humane endpoint, which was defined as noticeable extension of the abdomen, development of ascites, or body weight loss (>20%). In vivo fluorescence imaging was measured with an IVIS Lumina system (Caliper) weekly. Two mice were treated similarly to those in the adjuvant  $^{64}\text{Cu}$ -ipRIT group and euthanized on day 17 to observe tumor recurrence.

### Gemcitabine Treatment for Adjuvant Chemotherapy

For comparison, an in vivo study of adjuvant chemotherapy with gemcitabine (Sigma) was performed in the same model. The mice with orthotopic xPA-1-DC xenografts were randomized into 2 groups at 7 d after cell inoculation: adjuvant chemotherapy with gemcitabine and surgery-only control groups (10/group). One day after the surgical resection of PC, the mice were injected intraperitoneally with gemcitabine (100 mg/kg on days 0, 7, and 14; gemcitabine group) or saline (days 0, 7, and 14; surgery-only control group). The dose and timing of gemcitabine treatment were based on the previous studies (3,4,22). An evaluation similar to that for  $^{64}\text{Cu}$ -ipRIT was performed.

### Median Survival Time (MST)

In the in vivo treatment study, MST was determined for each treatment, and the percentage of increase in MST (treatment) was calculated as  $[\text{MST of treatment group}/\text{MST of the surgery-only control group} \times 100]$  (%) for  $^{64}\text{Cu}$ -ipRIT and gemcitabine.

### Statistical Analysis

Data are expressed as the mean  $\pm$  SD. *P* values were calculated using the Mann–Whitney *U* test for comparisons between 2 groups or the Kruskal–Wallis test with the Dunn post hoc test for comparisons among multiple groups, since the data were nonparametric. Differences in survival were evaluated using the log-rank test. All statistical analyses were conducted with a significance level of  $P < 0.05$ .

## RESULTS

### Establishment of the Resectable Human PC xPA-1-DC Orthotopic Xenograft Mouse Model

To investigate the utility of adjuvant  $^{64}\text{Cu}$ -ipRIT with  $^{64}\text{Cu}$ -PCTA-cetuximab in PC, we generated an orthotopic xenograft model with xPA-1-DC cells (Supplemental Fig. 1; supplemental materials are available at <http://jnm.snmjournals.org>). Immunohistochemistry confirmed EGFR overexpression in the xPA-1-DC orthotopic xenografts (Supplemental Fig. 2). At 9 d after tumor cell inoculation, primary tumors were located in the tail of the pancreas in all animals (Fig. 1A). We also observed hepatic metastasis (2/5 mice, 40%) and peritoneal dissemination (5/5 mice, 100%) at this time point (Fig. 1A). Therefore, we decided that 9 d after inoculation was too late for the surgery. At 7 d after tumor cell inoculation, we observed primary pancreatic tumors in all animals (Fig. 1B), but no obvious metastatic lesions were detected at any distant site. Given that the observations at 7 d after tumor cell inoculation apparently reproduced the clinical PC prognosis after surgery, we decided to perform partial pancreatectomy and splenectomy using the procedures shown in Figure 1C at this time point. Histologic observation revealed that tumor cells were invading the boundary of the normal pancreas surrounding the tumor xenograft (Supplemental Fig. 3). Therefore, we resected PCs with some margins. The presence of primary tumors was confirmed in all resected pancreases (Supplemental Fig. 4). In tumor-free mice that underwent partial pancreatectomy and splenectomy, the general condition and body weight were unperturbed (Supplemental Fig. 5).

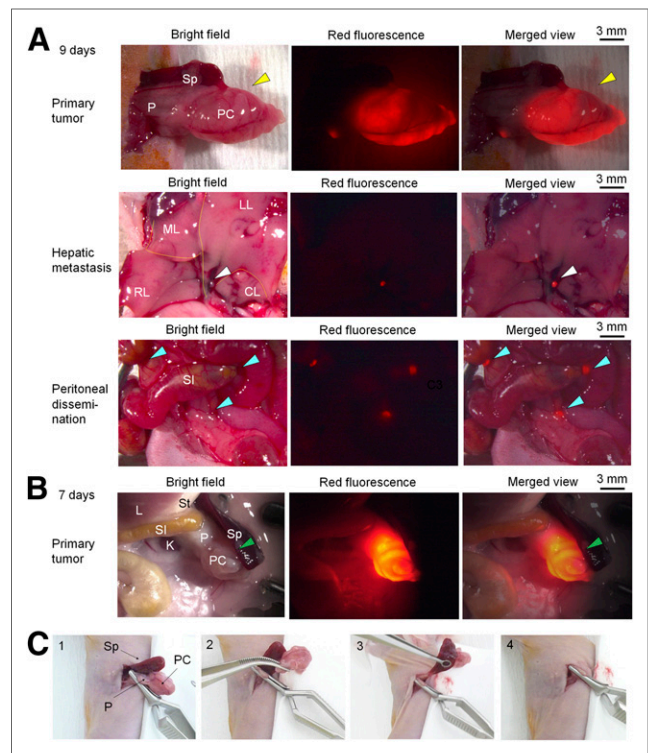


**FIGURE 1.** Mouse model with xPA-1-DC orthotopic PC xenografts. (A) Representative images of primary tumor located in tail of pancreas (yellow arrowheads), hepatic metastasis (white arrowheads), and peritoneal dissemination (blue arrowheads) at 9 d after tumor cell inoculation. (B) Representative images of primary tumor located in tail of pancreas at 7 d after tumor cell inoculation (green arrowheads). (C) Surgical procedures of partial pancreatectomy and splenectomy. Pancreas with tumor and spleen were gently exteriorized (1). Portion of pancreas with tumor and spleen was resected after ligation with clamp to prevent bleeding (2 and 3). Pancreas was returned to abdomen (4). CL, LL, ML, RL = caudate, left, median, and right lobes of liver, respectively; K = kidney; L = liver; P = pancreas; SI = small intestine; Sp = spleen; St = stomach.

### Postoperative Recurrence in xPA-1-DC Orthotopic Xenograft Mice

Two weeks after surgery, local recurrence (3/9 mice, 33%) (Fig. 2A, green arrowhead), hepatic metastasis (1/9 mice, 11%) (Fig. 2B, white arrowhead), and peritoneal dissemination (9/9 mice, 100%) (Fig. 2A, blue and yellow arrowheads; Fig. 2C, pink arrowhead) were observed (Supplemental Table 1). These lesions were histologically confirmed as tumors, namely local recurrence within the pancreas (Fig. 2D, green arrowhead) and metastatic lesions in the mesentery near the small intestine (Fig. 2D, yellow arrowhead), the peritoneum near the surgical sites (Fig. 2D, blue arrowhead), the liver (Fig. 2D, white arrowhead), and fatty tissue near the ovary (Fig. 2D, pink arrowhead). Distant metastases to other sites were not observed. These results indicated that this model reproduced the mode of postoperative recurrence seen in PC patients (2).

### Determination of the Therapeutic Dose for $^{64}\text{Cu}$ -ipRIT with $^{64}\text{Cu}$ -PCTA-Cetuximab

The dose–effect relationship for intraperitoneally injected  $^{64}\text{Cu}$ -PCTA-cetuximab was investigated. Treatment with 37 and 74 MBq of  $^{64}\text{Cu}$ -PCTA-cetuximab significantly reduced the percentage body weight relative to the initial value at day 3 after the

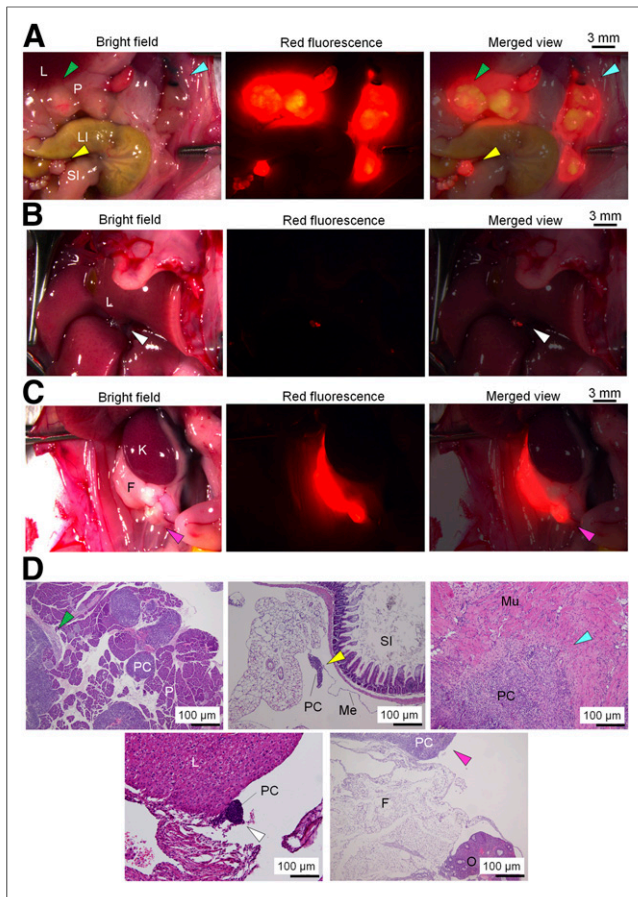


**FIGURE 2.** Postoperative recurrence at 2 wk after surgical resection of primary PC in mice with xPA-1-DC orthotopic xenografts. (A–C) Representative images of local recurrence (green arrowheads), hepatic metastasis (white arrowheads), and peritoneal dissemination (blue, yellow, and pink arrowheads) obtained with stereoscopic fluorescence microscope. (D) Histologic observations with hematoxylin and eosin staining of recurrent lesions presented in A–C. Color of arrowheads indicates similar recurrent lesions in A–C. F = fatty tissue; K = kidney; L = liver; LI = large intestine; Me = mesentery; Mu = muscle; O = ovary; P = pancreas; SI = small intestine.

injection compared with that of the control (0 MBq;  $P = 0.004$  and  $0.003$ , respectively), although no significant differences were observed at any other time points (Fig. 3A; Supplemental Table 2). For other treatment groups (11.1 and 22.2 MBq), there were no significant differences in percentage body weight at any time points compared with the control (0-MBq group). In addition,  $^{64}\text{Cu}$ -PCTA-cetuximab administration with 37 and 74 MBq significantly reduced white blood cell counts after intraperitoneal injection (day 7 in the 37-MBq group and days 7 and 14 in the 74-MBq group compared with those on day 0 in each group;  $P = 0.011$ ,  $0.016$ , and  $0.012$ , respectively; Fig. 3B, left). Significant reductions of platelet counts were observed in these 2 groups (day 14 in the 37-MBq group and day 7 in the 74-MBq group vs. day 0 in each group;  $P = 0.012$  and  $0.012$ , respectively; Fig. 3B, right). There were no significant differences in red blood cell counts (Fig. 3B, middle) or in any of the examined biochemical parameters (Fig. 3C). These data demonstrated that adverse effects of  $^{64}\text{Cu}$ -PCTA-cetuximab were dose-dependent, and the dose of 22.2 MBq was selected as the maximum tolerated dose as it did not cause any significant adverse changes in body weight or

hematologic and biochemical parameters in the mice after intraperitoneal administration. In addition, the tumor uptake of the xPA-1-DC orthotopic xenografts was confirmed before the in vivo treatment, showing a high tumor uptake of  $14.6 \pm 3.2$  percentage injected dose per gram (Supplemental Fig. 6), similar to that observed in HCT116-RFP xenografts (8).

#### Adjuvant $^{64}\text{Cu}$ -ipRIT with $^{64}\text{Cu}$ -PCTA-Cetuximab

Survival was significantly extended in the adjuvant  $^{64}\text{Cu}$ -ipRIT group compared with that in the surgery-only control group ( $P < 0.001$ ; Fig. 4). MST values in the adjuvant  $^{64}\text{Cu}$ -ipRIT and surgery-only control groups were 52.5 and 13.0 d, respectively, and  $^{64}\text{Cu}$ -ipRIT %MST was 403.8% (Supplemental Table 3). All mice in the surgery-only control group were dead before day 20. In contrast, we observed 100% survival at day 20 and 40% survival at day 83 in mice treated with adjuvant  $^{64}\text{Cu}$ -ipRIT (4/10 mice). No mice in any group showed a decrease in body weight over 20% relative to the initial body weight until the experimental endpoint. In vivo fluorescent imaging showed that tumor growth was inhibited in the adjuvant  $^{64}\text{Cu}$ -ipRIT group but not in the surgery-only control group (Fig. 5A). The mice that underwent adjuvant  $^{64}\text{Cu}$ -ipRIT had

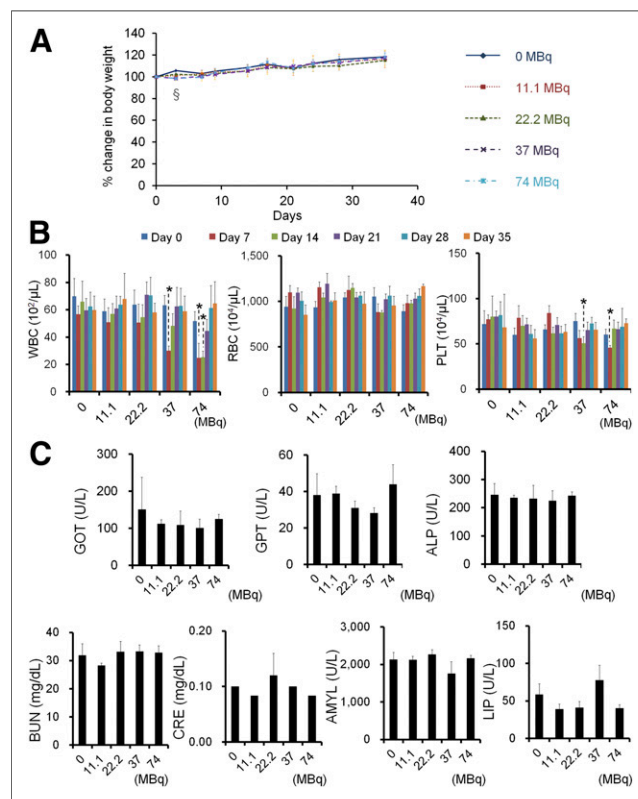


**FIGURE 3.** Toxicity of intraperitoneally injected  $^{64}\text{Cu}$ -PCTA-cetuximab.  $^{64}\text{Cu}$ -PCTA-cetuximab in 5-step doses was intraperitoneally injected in tumor-free mice (4–5/group). Values are mean  $\pm$  SD. (A) Percentage change in body weight for 35 d after  $^{64}\text{Cu}$ -PCTA-cetuximab injection.  $^{\S}$ Significant reductions in body weight in 37- and 74-MBq groups vs. 0-MBq group at day 3 ( $P < 0.05$ ). (B) Hematologic toxicity. Shown are numbers of white blood cells (WBCs), red blood cells (RBCs), and platelets (PLT) before (day 0) and after injection.  $^*P < 0.05$  vs. day 0 in each group. (C) Biochemical parameters at day 35 after injection; none showed significant changes. ALP = alkaline phosphatase; AMYL = amylase; BUN = blood urea nitrogen; CRE = creatinine; GOT = glutamate oxaloacetate transaminase; GPT = glutamate pyruvate transaminase; LIP = lipase.

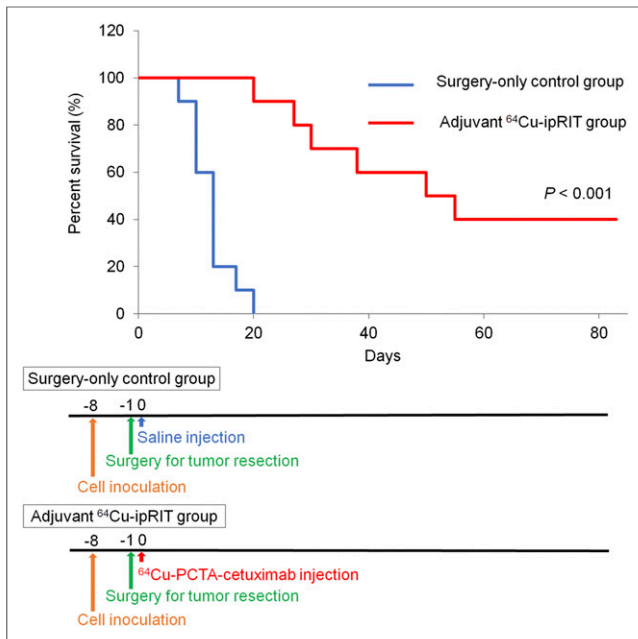


**FIGURE 4.** After surgical resection of PC in xPA-1-DC orthotopic xenograft mice, survival curves for adjuvant  $^{64}\text{Cu}$ -ipRIT with  $^{64}\text{Cu}$ -PCTA-cetuximab and surgery-only control groups (top), and treatment schedule (bottom) (10/group). Survival differed significantly between groups ( $P < 0.001$ ).

no detectable recurrent lesions in the pancreas or at any distant sites at day 17 (Fig. 5B). The 4 surviving mice in the adjuvant  $^{64}\text{Cu}$ -ipRIT group had no detectable tumor lesions at day 83.

#### Adjuvant Chemotherapy with Gemcitabine

To compare the effect of adjuvant  $^{64}\text{Cu}$ -ipRIT with  $^{64}\text{Cu}$ -PCTA-cetuximab to the conventional treatment, the efficacy of adjuvant chemotherapy with gemcitabine was also evaluated in the same model. Survival in the gemcitabine treatment group was nominally higher than that in the surgery-only control group, but the effect did not reach statistical significance ( $P = 0.185$ ; Fig. 6). MST values in the gemcitabine treatment and surgery-only control groups were 17.0 and 15.0 d, respectively, and %MST (gemcitabine) was 113.3% (Supplemental Table 3). In both the gemcitabine treatment and the surgery-only control groups, no mice showed body weight loss below 20% of the initial body weight until the experimental endpoint.

#### DISCUSSION

The adjuvant  $^{64}\text{Cu}$ -ipRIT with  $^{64}\text{Cu}$ -PCTA-cetuximab significantly prolonged survival by inhibiting tumor expansion without significant adverse events after surgical resection of PC, whereas adjuvant chemotherapy with gemcitabine did not significantly improve survival in an orthotopic mouse model. These results are in line with our previous study (8) but further demonstrated the efficacy of the adjuvant  $^{64}\text{Cu}$ -ipRIT with  $^{64}\text{Cu}$ -PCTA-cetuximab using a more clinically relevant orthotopic PC xenograft model that not only developed primary tumors but also reproduced local recurrence, hepatic metastasis, and peritoneal dissemination after surgery, as seen in PC patients.  $^{64}\text{Cu}$ -ipRIT and gemcitabine %MST values were 403.8% and 113.3%, respectively, indicating 3.4-fold higher efficacy of  $^{64}\text{Cu}$ -ipRIT. Adjuvant  $^{64}\text{Cu}$ -ipRIT suppressed

local recurrence in the pancreas and metastases at distant sites as 40% of the mice successfully survived without any detectable local recurrence and metastasis for 83 d. Considering that in the absence of adjuvant therapy, local recurrence, hepatic metastasis, and peritoneal dissemination were observed in, respectively, 33%, 11%, and 100% of animals at 2 wk after surgery in this model (Supplemental Table 1) and that the recurrence rate is 80%–85% after surgery in PC patients (21), the 40% survival without recurrence after adjuvant  $^{64}\text{Cu}$ -ipRIT with  $^{64}\text{Cu}$ -PCTA-cetuximab warrants further development of this therapy for future clinical use.

Preclinical studies have demonstrated that intraperitoneal, rather than intravenous, administration of radiolabeled antibodies resulted in their high and rapid accumulation in pancreatic tumors, liver metastasis, and peritoneal dissemination in vivo (8–10). Furthermore, xPA-1-DC orthotopic xenografts exhibited high tumor uptake of  $^{64}\text{Cu}$ -PCTA-cetuximab (percentage injected dose per gram,  $14.6 \pm 3.2$ ; Supplemental Fig. 6) after intraperitoneal administration. These data suggest that intraperitoneally administered  $^{64}\text{Cu}$ -PCTA-cetuximab reaches the invisible small lesions in the peritoneal cavity as well as in the pancreas and liver, resulting in better survival without recurrence. Previous studies have demonstrated that intraperitoneally administered drugs are delivered to the pancreas via the lymphatic system (23) and to the liver via the portal vein (24). This suggests the rationale for using  $^{64}\text{Cu}$ -PCTA-cetuximab after intraperitoneal administration as an effective approach to prevent local recurrence, hepatic metastasis, and peritoneal dissemination in PC. Considering the limited distribution of

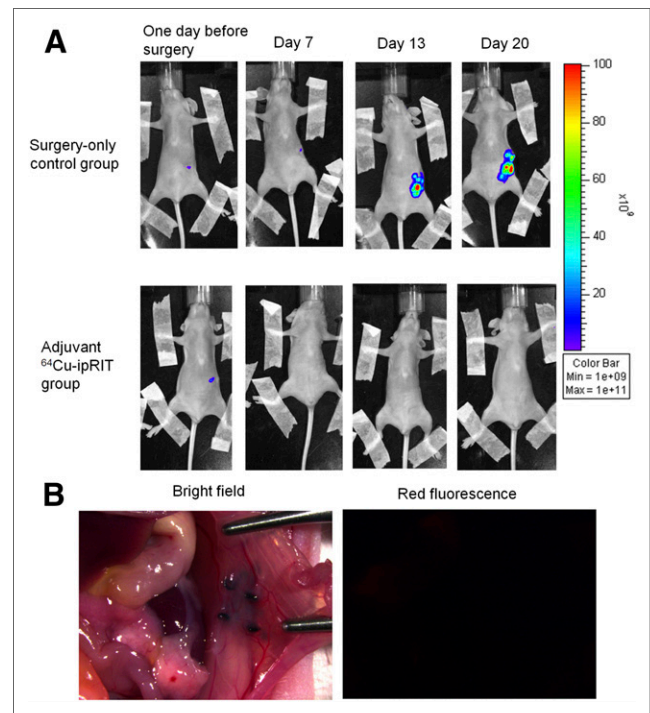


**FIGURE 5.** Observations during in vivo treatment. (A) Representative in vivo fluorescence images of mice from adjuvant  $^{64}\text{Cu}$ -ipRIT with  $^{64}\text{Cu}$ -PCTA-cetuximab group and surgery-only controls. (B) Representative stereoscopic bright-field and fluorescence microscope images at day 17 in mouse that underwent adjuvant  $^{64}\text{Cu}$ -ipRIT with  $^{64}\text{Cu}$ -PCTA-cetuximab. There were no detectable recurrent lesions in pancreas or at any distant site.

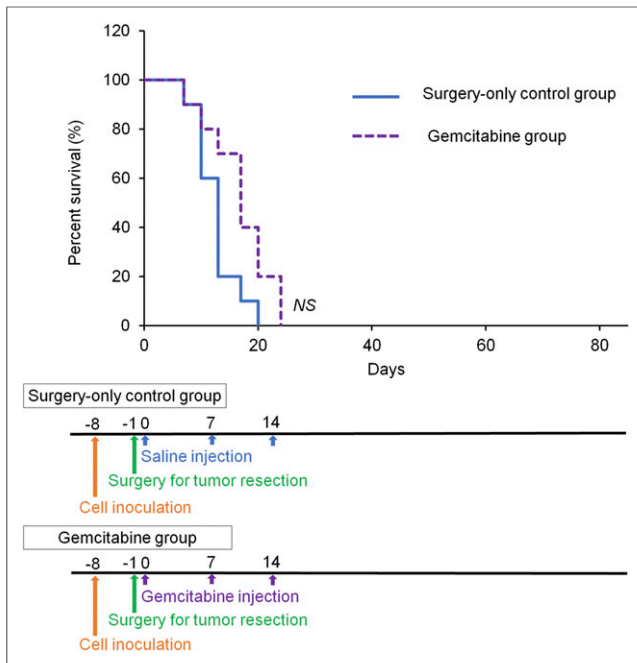


**FIGURE 6.** After surgical resection of PC in xPA-1-DC orthotopic xenograft mice, survival curves for adjuvant chemotherapy with gemcitabine and surgery-only control groups (top), and treatment schedule (bottom) (10/group). NS = not significant.

cetuximab in large tumor masses, especially distant from blood vessels or the surface ( $>100\ \mu\text{m}$ ) (25), and the short radiation range of  $^{64}\text{Cu}$  in tissues (mean range  $<1\ \text{mm}$ ;  $0.02\text{--}10\ \mu\text{m}$  for Auger electrons (15)), the  $^{64}\text{Cu}$ -ipRIT with  $^{64}\text{Cu}$ -PCTA-cetuximab would be effective in cases involving small lesions rather than large tumor masses. Radioimmunotherapy with Auger electrons reportedly causes cytotoxicity to tumor cells by damaging the cell membrane, similar to damaging the nucleus (26). This might explain the effectiveness of  $^{64}\text{Cu}$ -ipRIT. In this study, adjuvant chemotherapy with gemcitabine tended to prolong survival, but the effect was not statistically significant. These data are consistent with the outcome of phase III studies that showed a limited survival benefit of gemcitabine to patients after surgery (3,4).

Cetuximab has high binding affinity for EGFR, which is highly expressed in a wide variety of cancers, including PC (19). Previous studies have reported that a high proportion ( $\leq 90\%$ ) of PCs shows EGFR overexpression (19). In PC patients, *EGFR* gene amplification is increased (41%), whereas EGFR ectodomain mutations that prevent cetuximab binding are rare (1.5%) (27). This evidence led us to explore whether the use of adjuvant  $^{64}\text{Cu}$ -ipRIT with  $^{64}\text{Cu}$ -PCTA-cetuximab targeting EGFR could be effective for many PC patients.

This study has several limitations. We used mice with orthotopic xenografts to evaluate the efficacy of the adjuvant therapy for PC. Although this model reproduced the clinical prognosis well, lung and bone metastases that have been observed in some PC patients (2) are not manifested in this model. Moreover, *KRAS* mutations, which attenuate the effectiveness of molecular targeted therapy with cetuximab because of the impairment of *KRAS* signaling (28), are present in 49% of PC patients (27). Because we previously demonstrated that  $^{64}\text{Cu}$ -ipRIT with  $^{64}\text{Cu}$ -PCTA-cetuximab was effective against gastrointestinal tumors expressing EGFR with or without *KRAS* mutations (8), the effect in *KRAS*-mutant PC would be

expected. However, in this study, we used only 1 cell line (xPA-1) expressing wild-type *KRAS* (29). Therefore, further studies using *KRAS*-mutant cell lines and patient-derived xenografts would be helpful to understand the clinical application of this therapy. Additionally, there might be discrepancies between mice and humans in the immunoreactivity of  $^{64}\text{Cu}$ -PCTA-cetuximab. Therefore, careful dose optimization will be necessary in humans. In this study, a single administration of  $^{64}\text{Cu}$ -PCTA-cetuximab significantly prolonged survival in the mouse model; thus, multiple dosages might be worth investigating in future studies to improve the outcome.

## CONCLUSION

We demonstrated that adjuvant  $^{64}\text{Cu}$ -ipRIT with  $^{64}\text{Cu}$ -PCTA-cetuximab after surgical resection of PC effectively prolonged the survival, exhibited minimal toxicity, and was associated with an overall better outcome than that after conventional adjuvant chemotherapy with gemcitabine in a mouse orthotopic xenograft model. This therapy effectively suppressed the local recurrence, hepatic metastasis, and peritoneal dissemination that usually underlie the poor prognosis of PC patients. Our findings suggest that adjuvant  $^{64}\text{Cu}$ -ipRIT with  $^{64}\text{Cu}$ -PCTA-cetuximab can be a novel treatment option to improve the condition of PC patients after surgery.

## DISCLOSURE

This work was supported by KAKENHI grant 16K10375 from the Japan Society for the Promotion of Science. Hiroki Matsumoto is an employee of Nihon Medi-Physics Co., Ltd. No other potential conflict of interest relevant to this article was reported.

## ACKNOWLEDGMENT

We thank Hisashi Suzuki (QST) for providing  $^{64}\text{Cu}$ .

## KEY POINTS

**QUESTION:** The purpose of this study was to investigate the efficacy of  $^{64}\text{Cu}$ -intraperitoneal radioimmunotherapy (ipRIT) with  $^{64}\text{Cu}$ -labeled antiepidermal growth factor receptor antibody cetuximab in vivo to provide an effective adjuvant treatment after pancreatic cancer (PC) surgery.

**PERTINENT FINDINGS:** Adjuvant  $^{64}\text{Cu}$ -ipRIT with  $^{64}\text{Cu}$ -labeled cetuximab after PC surgery significantly prolonged survival with minimal toxicity and showed an overall better outcome than conventional adjuvant chemotherapy with gemcitabine in a clinically relevant preclinical model. This therapy effectively suppressed local recurrence, hepatic metastasis, and peritoneal dissemination that usually underlie the poor prognosis of PC patients.

**IMPLICATIONS FOR PATIENT CARE:**  $^{64}\text{Cu}$ -ipRIT with  $^{64}\text{Cu}$ -labeled cetuximab can be an effective adjuvant therapy to improve the prognosis of PC patients after surgery.

## REFERENCES

1. Siegel RL, Miller KD, Jemal A. Cancer statistics, 2015. *CA Cancer J Clin*. 2015;65:5–29.
2. Nakao A, Fujii T, Sugimoto H, et al. Oncological problems in pancreatic cancer surgery. *World J Gastroenterol*. 2006;12:4466–4472.
3. Oettle H, Neuhaus P, Hochhaus A, et al. Adjuvant chemotherapy with gemcitabine and long-term outcomes among patients with resected pancreatic cancer: the CONKO-001 randomized trial. *JAMA*. 2013;310:1473–1481.

4. Ueno H, Kosuge T, Matsuyama Y, et al. A randomised phase III trial comparing gemcitabine with surgery-only in patients with resected pancreatic cancer: Japanese study group of adjuvant therapy for pancreatic cancer. *Br J Cancer*. 2009;101:908–915.
5. Kinuya S, Yokoyama K, Fukuoka M, et al. Intraperitoneal radioimmunotherapy to treat the early phase of peritoneal dissemination of human colon cancer cells in a murine model. *Nucl Med Commun*. 2007;28:129–133.
6. Borchardt PE, Yuan RR, Miederer M, et al. Targeted actinium-225 in vivo generators for therapy of ovarian cancer. *Cancer Res*. 2003;63:5084–5090.
7. Koppe MJ, Bleichrodt RP, Soede AC, et al. Biodistribution and therapeutic efficacy of  $^{125/131}\text{I}$ -,  $^{186}\text{Re}$ -,  $^{88/90}\text{Y}$ -, or  $^{177}\text{Lu}$ -labeled monoclonal antibody MN-14 to carcinoembryonic antigen in mice with small peritoneal metastases of colorectal origin. *J Nucl Med*. 2004;45:1224–1232.
8. Yoshii Y, Yoshimoto M, Matsumoto H, et al. Integrated treatment using intraperitoneal radioimmunotherapy and positron emission tomography-guided surgery with  $^{64}\text{Cu}$ -labeled cetuximab to treat early- and late-phase peritoneal dissemination in human gastrointestinal cancer xenografts. *Oncotarget*. 2018; 9:28935–28950.
9. Wu ST, Williams CD, Grover PA, Moore LJ, Mukherjee P. Early detection of pancreatic cancer in mouse models using a novel antibody, TAB004. *PLoS One*. 2018;13:e0193260.
10. Rivoire ML, Yoshida K, Voiglio EJ, et al. Intraportal injection of monoclonal antibody in nude mice bearing hepatic metastases. *J Surg Oncol*. 1993;54: 71–77.
11. Dash A, Pillai MR, Knapp FF. Production of  $^{177}\text{Lu}$  for targeted radionuclide therapy: available options. *Nucl Med Mol Imaging*. 2015;49:85–107.
12. *Nuclear Medicine in Thyroid Cancer Management: A Practical Approach*. Vienna, Austria: IAEA; 2009:288. IAEA-TECDOC-1608.
13. Apostolidis C, Molinet R, McGinley J, et al. Cyclotron production of Ac-225 for targeted alpha therapy. *Appl Radiat Isot*. 2005;62:383–387.
14. Ohya T, Nagatsu K, Suzuki H, et al. Efficient preparation of high-quality  $^{64}\text{Cu}$  for routine use. *Nucl Med Biol*. 2016;43:685–691.
15. Lewis J, Laforest R, Buettner T, et al. Copper-64-diacetyl-bis( $N^4$ -methylthiosemicarbazone): an agent for radiotherapy. *Proc Natl Acad Sci USA*. 2001;98: 1206–1211.
16. Capasso E, Valentini MC, Mirzaei S, et al. Radionuclide treatment with  $^{64}\text{Cu}$ -Cl<sub>2</sub> in patients with progressive malignant gliomas [abstract]. *Eur J Nucl Med Mol Imaging*. 2015;42(suppl 1):S12.
17. Guo Y, Parry JJ, Laforest R, Rogers BE, Anderson CJ. The role of p53 in combination radioimmunotherapy with  $^{64}\text{Cu}$ -DOTA-cetuximab and cisplatin in a mouse model of colorectal cancer. *J Nucl Med*. 2013;54:1621–1629.
18. Song IH, Lee TS, Park YS, et al. Immuno-PET imaging and radioimmunotherapy of  $^{64}\text{Cu}$ -/ $^{177}\text{Lu}$ -labeled anti-EGFR antibody in esophageal squamous cell carcinoma model. *J Nucl Med*. 2016;57:1105–1111.
19. Oliveira-Cunha M, Newman WG, Siriwardena AK. Epidermal growth factor receptor in pancreatic cancer. *Cancers (Basel)*. 2011;3:1513–1526.
20. Yoshida C, Tsuji AB, Sudo H, et al. Therapeutic efficacy of c-kit-targeted radioimmunotherapy using  $^{90}\text{Y}$ -labeled anti-c-kit antibodies in a mouse model of small cell lung cancer. *PLoS One*. 2013;8:e59248.
21. Gürlevik E, Fleischmann-Mundt B, Brooks J, et al. Administration of gemcitabine after pancreatic tumor resection in mice induces an antitumor immune response mediated by natural killer cells. *Gastroenterology*. 2016;151:338–350.
22. Miyake K, Kiyuna T, Miyake M, et al. Patient-derived orthotopic xenograft models for cancer of unknown primary precisely distinguish chemotherapy, and tumor-targeting *S. typhimurium* A1-R is superior to first-line chemotherapy. *Signal Transduct Target Ther*. 2018;3:12.
23. Wang B, Sun C, Wang S, et al. Mouse dendritic cell migration in abdominal lymph nodes by intraperitoneal administration. *Am J Transl Res*. 2018;10:2859–2867.
24. Speyer JL, Sugarbaker PH, Collins JM, Dedrick RL, Klecker RW Jr, Myers CE. Portal levels and hepatic clearance of 5-fluorouracil after intraperitoneal administration in humans. *Cancer Res*. 1981;41:1916–1922.
25. Lee CM, Tannock IF. The distribution of the therapeutic monoclonal antibodies cetuximab and trastuzumab within solid tumors. *BMC Cancer*. 2010;10:255.
26. Pouget JP, Santoro L, Raymond L, et al. Cell membrane is a more sensitive target than cytoplasm to dense ionization produced by auger electrons. *Radiat Res*. 2008;170:192–200.
27. Lee J, Jang KT, Ki CS, et al. Impact of epidermal growth factor receptor (EGFR) kinase mutations, EGFR gene amplifications, and KRAS mutations on survival of pancreatic adenocarcinoma. *Cancer*. 2007;109:1561–1569.
28. Soulières D, Greer W, Magliocco AM, et al. KRAS mutation testing in the treatment of metastatic colorectal cancer with anti-EGFR therapies. *Curr Oncol*. 2010;17(suppl):S31–S40.
29. Logan-Collins J, Thomas RM, Yu P, et al. Silencing of RON receptor signaling promotes apoptosis and gemcitabine sensitivity in pancreatic cancers. *Cancer Res*. 2010;70:1130–1140.